Scientific paper

New Compounds Derived from Nitrophenol Synthesis, Structural Investigation and Anticorrosion Properties

Ali Mahdi Farhan,[1,*] Hanaa Kadtem Egzar[2] and Hawraa Mahdi Alabidi[2]

[1] *Ministry of Education, Al-Najaf, Iraq*

[2] *Department of Chemistry, College of Science- University of Kufa*

* *Corresponding author: E-mail: aliphd256@gmail.com*

Received: 10-03-2023

Abstract

A new azo compound **3** [2-((4-hydroxy-3-(*E*)-(2-hydroxy-5-nitrophenyl)diazenyl)benzaldehyde] and the azo-Schiff derivative **4** [2-((4-hydroxy-3-((*E*)-(2-hydroxy-5-nitrophenyl)diazenyl)benzylidene)amino)-4-nitrophenol[(azo-Schiff **4**) have been synthesized. ^{13}C-NMR, ^{1}H-NMR, FT-IR, mass spectroscopy and UV-Vis analysis was used to characterized new compounds. The new synthesized compound azo-Schiff **4** was utilized to inhibit mild steel (MS) corrosion at little concentrations (0.001–0.006 M). Weight loss measurements studies in 1 M HCl and at 298 K showed that azo-Schiff **4** has a good corrosion inhibition efficiency, 75% at 0.002 M of inhibitors. It was found that adsorption methods follow Langmuir isotherm with ΔG values around –23.8 kJ/mol; this confirms that a stable protective film is formed spontaneously during physical adsorption on the mild steel.

Keywords: Azo compounds, Schiff base, anticorrosion, spectral identification.

1. Introduction

In most manufacturing methods, hydrochloric acid (HCl) is utilized as a washing and cleaning solution to remove rust from mild steel (MS). The acidic medium causes the evolution of hydrogen and formation of chloride ions dissolved in water, which accelerate corrosion. To prevent the effect of the HCl acid, effective and influential additives are added to protect the surfaces of the alloys and metals from corrosion.[1–3] Among the most often used inhibitors to protect metals from the effects of acids are organic inhibitors because they are some of the most effective, practical, efficient and low-cost techniques.[4] Organic inhibitors, for example those containing conjugate π bonds, aromatic nuclei, and heteroatoms (oxygen, nitrogen, carbon or sulfur), are one of the broadly utilized inhibitors used to the resist metal corrosion.[5–12] Organic inhibitors lower the rate of metal corrosion by inhibiting the active sites when the inhibitor is adsorbed on the metal surface thus creating a protective barrier between the electrolyte and the metal surface that displaces water molecules.[13,14] Studies have shown the effectiveness of Schiff bases in inhibiting corrosion in an acidic medium because of its –C=N– group. The π-bond in –C=N– group is able to interact with surface of the metal and nitrogen atoms are capable to form coordinate covalent bonds by its unshared electrons.[15,16] Azo compounds are used as corrosion inhibitors due to their ability to form a protective layer and a chelating complex with the surface of the metal due to the presence of an active group (–N=N–).[17–20]

A number of researchers already synthesized new azo compounds and tested them as anticorrosion chemicals. For example, a new azo-coumarin dye was created by Yusoff et al.,[21] and it was discovered that the new compounds work well as anticorrosion agents. On the other hand, Schiff base compounds are also used as anticorrosion chemicals. For instance, Madani et al.[22] prepared two Schiff base compounds from benzidine and found that these compounds, even at low concentrations, showed a good inhibitory action in the tested medium and that the increase in inhibitors concentrations increased the effectiveness of their inhibition activity. Because of this, our work included developing novel azo-Schiff compounds derived from nitrophenol compounds and screening them for anticorrosion properties to obtain promising results in this area.

2. Experimental Part

2. 1. Materials and Instruments

All organic chemical, solvents and inorganic salts these utilized in this work were provided by Merck, Sigma Aldrich, Fluka, and BDH.

Mass spectra were measured by AB SCIEX (3200) Mass analyzer, UV-Vis spectra were measured in ethanol using a Shimadzu UV-1650 instrument (Japan) and IR spectra were obtained as KBr disks using a Shimadzu FT-IR 8400 instrument in the range 400–4000 cm^{-1}. ^{1}H-NMR spectra of ligand were recorded by using Bruker Avance-111 (300 MHz) spectrometer using DMSO-d_6 as the solvent for measurement; chemical shifts are given relative to the internal standard tetramethylsilane (TMS). Melting points were determined using a melting point apparatus.

Mild steel plates (1 cm × 1 cm × 0.1 cm) were used for weight loss. The plates were washed with acetone , distilled water and desiccated prior any experiment. The HCl solution was utilized with concentration of 1 M as corrosive medium.

2. 2. Synthesis of Azo Compound 3[23,24]

To obtain the azo compound **3**, 2-amino-4-nitrophenol (**1**) (154 mg, 0.01 mmol) was dissolved in 25 mL of absolute ethanol. After adding 2 mL of concentrated HCl, following 25 minutes of stirring in an ice bath, 25 mL of an ice-cold sodium nitrite solution, $NaNO_2$ (10%) was added drop wise, over the time of 35 minutes. The reaction mixture became reddish brown and was added drop by drop to a second ice-cold solution of 3-hydroxybenzaldehyde (**2**) (122 mg, 0.01 mmol) in 20 mL of alkaline ethanol, which was then stirred continuously at 45 °C overnight. The reaction mixture was neutralized using diluted ammonia and hydrochloric acid until pH 7, then the target product was washed in cold distilled water, filtrated and dried.

Yield: 350 mg (74%), deep brown powder, m.p.< 300 °C, FT-IR (KBr) (cm^{-1}): 3396 (OH), 2929 and 2889 (C-H aliph), 2833 and 2752 (C-H aldehyde), 1674 (C=O, aldehyde), 1594 (C=C, arom), 1496 (N=N), 1308 and 1163 (NO_2). ^{1}H-NMR (300 MHz, DMSO-d_6) δ 9.43 (s, 1H, CHO), 8.51 (s, 1H, H3-arom A), 8.22 (s, 1H, OH- arom A), 8.19 (s, 1H, OH- arom B), 7.74–7.71 (d, 2H, H5-arom A + H2-arom B), 7.47 (s, 1H, H6-arom B), 6.43–6.42 (d, H3-arom B), 5.94–5.91 (d, H6-arom A).

2. 3. Synthesis of Azo-Schiff Base Compound 4[25,26]

Schiff base compound **4** was prepared by dissolving azo compound **3** (600 mg, 2.09 mmol) in 40 mL of ethanol containing 2-amino-4-nitrophenol (**1**) (321 mg, 2.09 mmol) and a few drops of glacial acetic acid; the mixture was heated under reflux for 7–9 hours. TLC was used to check the progress of the reaction (mobile phase: chloroform/methanol (3:1.5)). After cooling, the solid product that precipitated from the ethanol was collected by filtration, and purified by recrystallization to obtain the desired product.

Yield: 850 mg (82%), pale yellow powder, m.p. 271–273 °C, R_f 0.38, FT-IR (KBr) (cm^{-1}): 3402 (OH), 2918 and 2896 (C-H aliph), 1643 (C=N), 1594 (C=C, arom), 1498 (N=N), 1309 and 1161 (NO_2).^{13}C-NMR (75.5 MHz, DMSO-d_6) δ 155.9 (C=N), 138.3 (C-OH), 137.9 (C-NO_2), 130.4 (C1- arom B), 126.9 (C4- arom B),119.8 (C5- arom B), 117.2 (C3- arom A + C3- arom C), 115.9 (C2- arom A + C2- arom C), 115.2 (C5- arom A + C5- arom C), 113.7 (C2+5- arom B), 107.2 (C6- arom A + C6- arom C).

2. 4. Weight Loss Measurements

The gravimetric measurements were carried out for mild steel plates in 1 M HCl solution in the absence and presence of the azo-Schiff **4** solution. After washing and weighting, the MS plates were immersed in corrosive environment for 1080 h at 298 K, then the loss in weight was determined by the change in MS plate's weights. MS surface coverage (θ), rate of corrosion (*CR*) and efficiency of inhibition (*IE* %), were calculated by equations 1–3.

$$CR = \frac{W}{At} \quad (1)$$

$$IE\% = \frac{CR^\circ - CR}{CR^\circ} \times 100 \quad (2)$$

$$\theta = \frac{CR^\circ - CR}{CR^\circ} \quad (3)$$

Where A is the area of MS plates in cm^2, W represents the lost weight of MS plates in mg, CR is the rate of corrosion, and t is the time of immersion in h in the presence of azo-Schiff **4** solution.

3. Results and Discussion

3. 1. Characterization of Azo 3 and Schiff base 4 Compounds

A new azo compound **3** was successfully synthesized by the coupling reaction between 2-amino-4-nitrophenol (**1**) and 3-hydroxybenzaldehyde (**2**) in a basic medium as shown in scheme 1.

By using spectral methods such as FT-IR, the azo compound **3** was characterized, which showed clear bands absorption due to stretching vibration of functional groups, for instance, the band of the hydroxyl group was observed at 3396 cm^{-1}, while the carbonyl aldehyde absorbed at 1674 cm^{-1}; furthermore, the C–H of the aldehyde group appeared as a double band at 2833 and 2752 cm^{-1}; the other absorptions of the compound **3** are listed in Table 1.

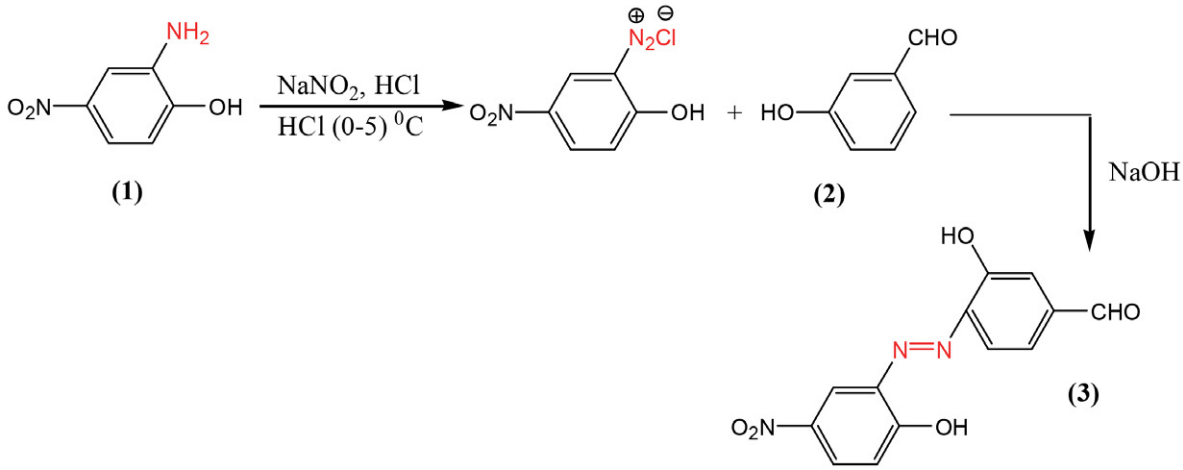

Scheme 1. Synthesis azo compound **3**.

Also, the new compound **3** was characterized by its ^{1}H-NMR spectrum, displaying a singlet at 9.43 ppm due to an aldehyde group proton, whereas the proton of the phenol group appeared at a chemical shift of 8.22 ppm, whereas the aromatic protons were observed at downfield in the range of 8.51–5.91 ppm as a result of the nitro group having electron withdrawing characteristics (Figure 1).

In the second step of the synthesis, Schiff base derivative **4** is prepared by reacting an azo molecule **3** with 2-amino-4-nitrophenol (**1**) in an acidic medium, as shown in Scheme 2.

In the FT-IR spectrum of the azo-Schiff derivative **4** new absorption bands belonging to azo-methane group appeared at 1643 cm^{-1}, also the stretching vibration of azo

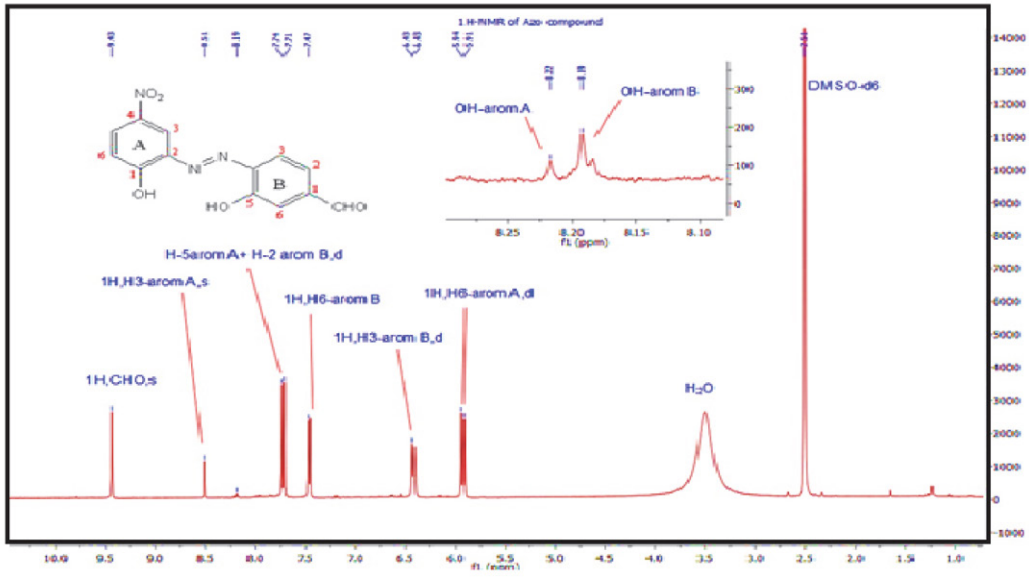

Figure 1. ^{1}H-NMR of azo compound **3**.

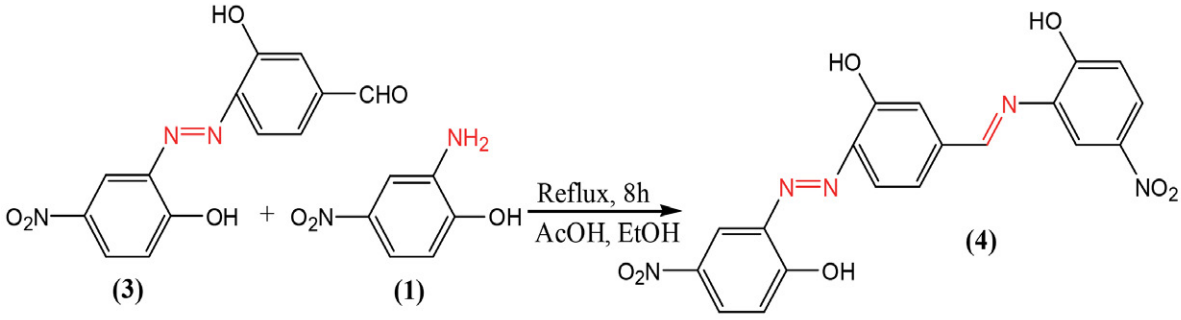

Scheme 2. Synthesis of the azo-Schiff derivative **4**.

group was observed at 1498 cm^{-1}, the other absorption bands of this compound are listed in Table 2.

The newly formed compound **4**, on the other hand, was identified by its ^{13}C-NMR spectrum, which also revealed a clear signal at 155.9 ppm caused by a resonant azo-methane group. The aromatic carbon atoms were observed in the range of 138.3–107.2 ppm as a result of the electronic effect of the neighboring group to the carbon atom (Figure 2).

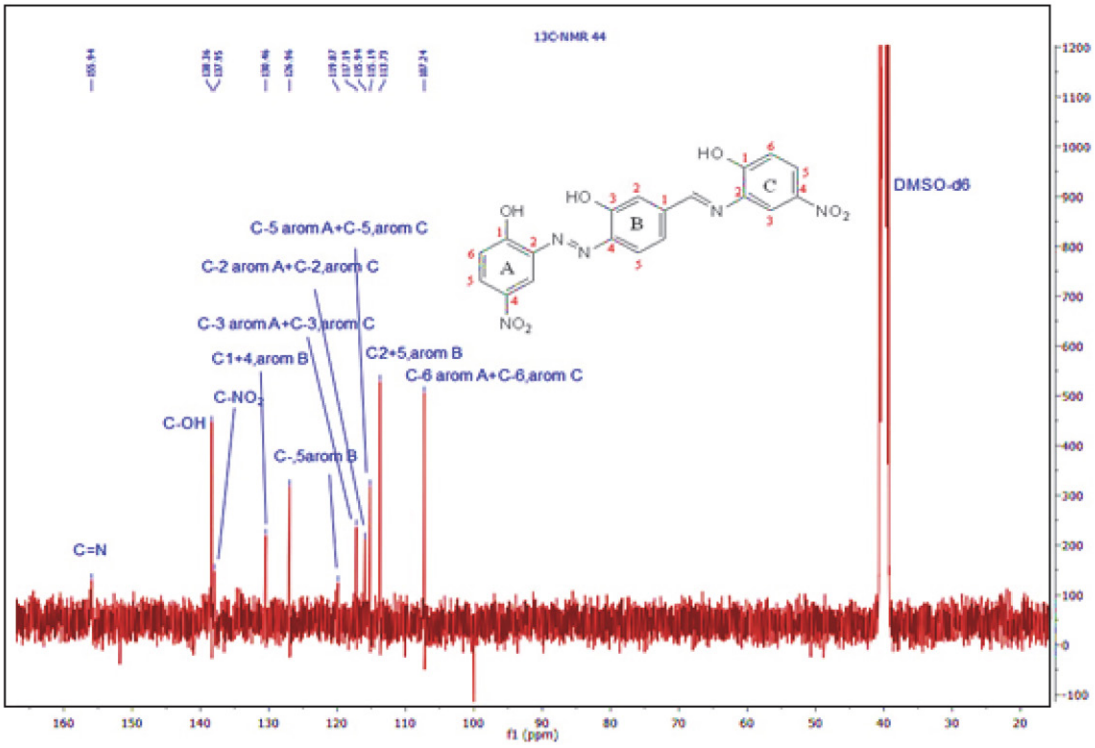

Figure 2. ^{13}C-NMR of azo-Schiff compound **4**.

Table 1. Characterization of azo compound **3** and azo-Schiff compound **4** by FT-IR

Compound	ν OH	ν C-H aliph	ν C-H aldehyde	ν C=O	ν C=N	NO_2
Azo compound	2290	2920	2833 – 2752	1574	–	1308 – 1163
Schiff compound	3402	2918	–	–	1643	1309 – 1161

3. 2. Mass Spectra

Mass spectrum for compound **3** showed a peak at *m/e* 285 confirming the molecular ion of the azo compound **3**, the primary fragmentation takes place in two ways, with the first route being the loss of N_2 of the azo group giving a peak at *m/e* 259; the other path starts by the elimination of two OH groups giving a peak at *m/e* 255 (Scheme 3).

3. 3. UV-Vis Spectrum

The electronic absorption spectra of the prepared compounds were measured in ethanol as the solvent. The essential absorption of the azo compound **3** and azo-Schiff derivative **4** appeared at 401 nm and 480 nm, respectively. The spectral data and some physical properties are listed in Table 2.

Table 2. Electronic spectral data of prepared compounds **3** and **4**.

Compound	color	Value of λ *max* (nm)	Type of transition
Azo compound **3**	Brown	286, 291	π–π*
		335	n-π*
		401	CT
Azo-Schiff base **4**	Dark brown	212,234	π–π*
		340	n-π*
		480	CT

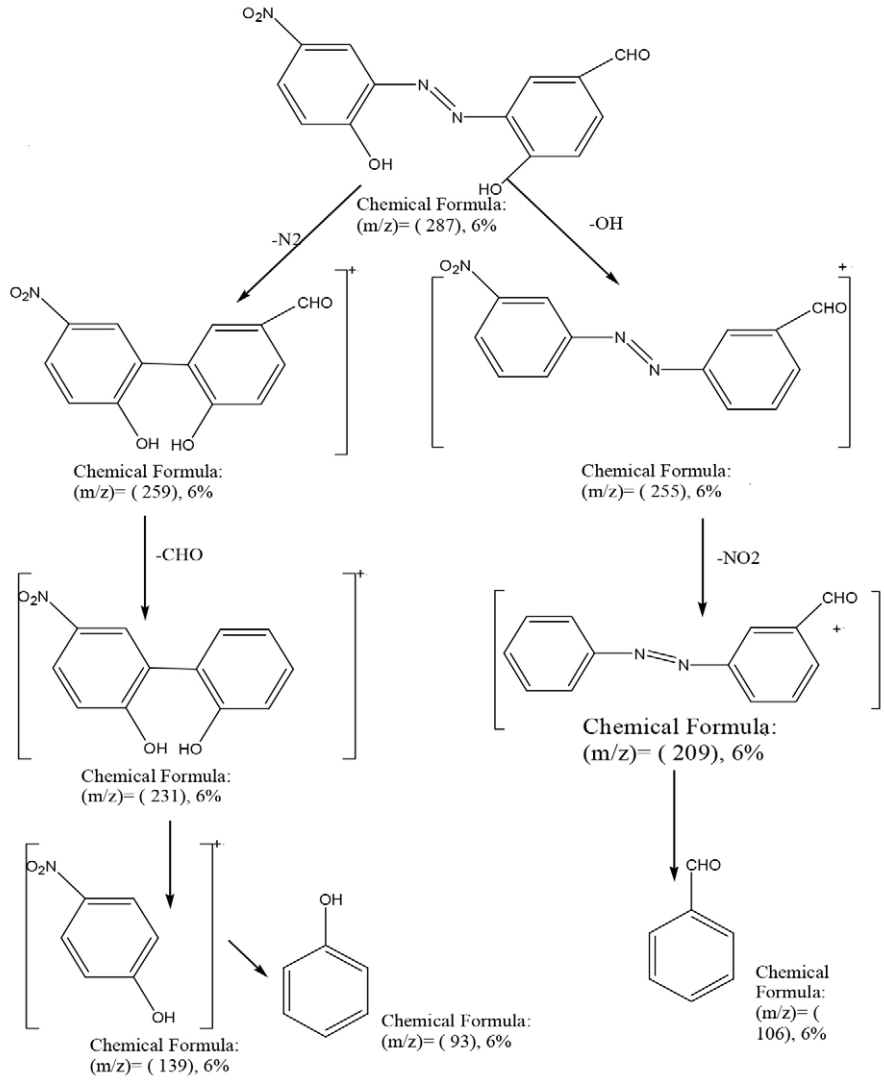

Scheme 3. A proposed pathway for MS fragmentation of the azo compound **3.**

3. 4. Gravimetric Measurements

Figures 3 and 4 demonstrate the weight loss results of MS plates in the presence and absence of the solution of azo-Schiff **4** in the acidic environment. The inhibition activity of azo-Schiff compound **4** to the corrosion of MS in 1 M HCl might be attributed to the existence of various groups having an evident effect on the inhibition efficiency produced by electron donating groups (–N=N–, HC=N, –OH); this adsorption centers (*i.e.* electron donating) increase adsorption and enhance the surface area covered by the compound and thus increase the efficiency of inhibition. Presences of –OH (electron donor) group in the azo-Schiff **4** enhanced the conjugation and facilitated bonding of the benzene ring. $-NO_2$ group in the azo-Schiff **4** decreases the inhibition efficiency, because of the electron withdrawing effect of nitro group, which decrease the electron density on the ring, and therefore the efficiency of the inhibition as well.[27]

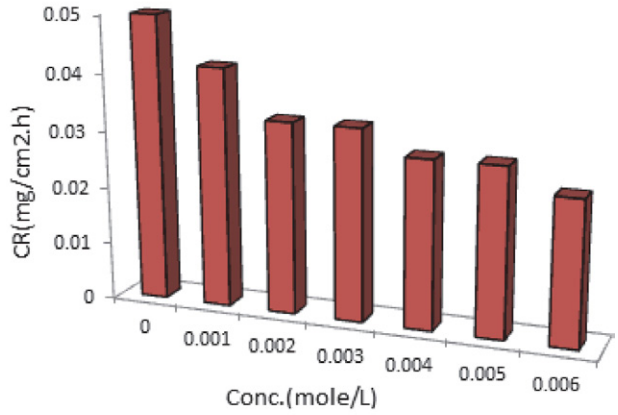

Figure 3. Effect of azo-Schiff **4** solution concentration on the corrosion rate of mild steel plates in 1 M HCl at 303 K.

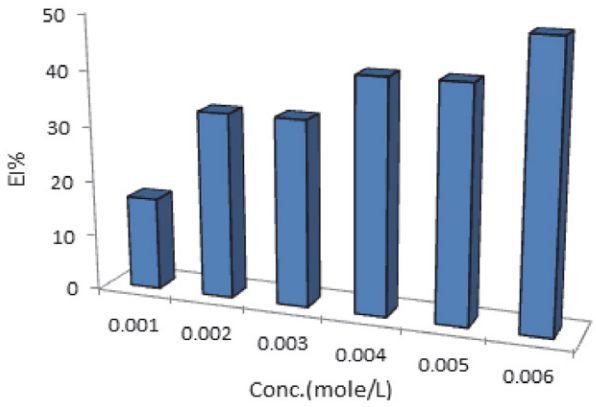

Figure 4. Influence of concentrations of azo-Schiff **4** solution on the efficiency of inhibition of MS plates corrosion in 1 M HCl at 298 K.

3. 5. Adsorption Isotherms

To find the most suitable and the best adsorption isotherm we used values of surface coverage (θ) that were obtained from the weight loss results (Figure 5). The adsorption isotherm assists to achieve the bonding between the surface of the plates and the azo-Schiff **4** molecules. The azo-Schiff **4** molecules are adsorbed physically or chemically on the surface of the plates. To recognize the adsorption type, the isothermal adsorption Freundlich, Temkin, and Langmuir isotherms were applied to methodological results. It was noticed that the mechanism of adsorption of azo-Schiff **4** on the MS surfaces obeyed Langmuir adsorption isotherm as shown by the high value of the regression coefficient (R^2 = 0.9295) indicating a good fitting; the obtained values of the intercept and slope were 0.0042 and 1.3888, respectively; the slope value being close to the unity thus suggesting a homogenous distribution and monolayer coverage of the azo-Schiff **4** molecules on the surface as supposed by Langmuir equation.

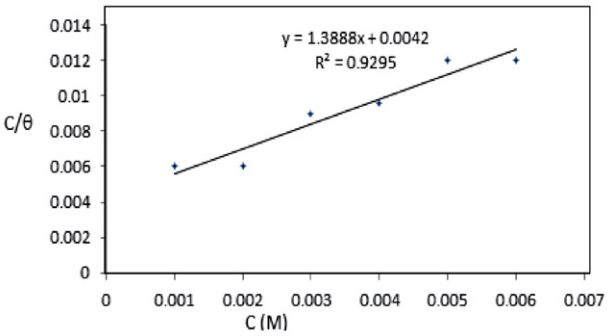

Figure 5. Langmuir isotherm of MS plates in the presence of the azo-Schiff **4**.

The value of the adsorption equilibrium constant (K_{ads}) equals 234.09; it was obtained from the straight line of C/θ and concentrations (C) as shown in the Equation 4.

$$\frac{C}{\theta} = \frac{1}{K_{ads.}} + C \quad (4)$$

To find the value of the adsorption free energy (ΔG_{ads}) we used the Equation 5.

$$\Delta G_{ads} = -RTln55.5K_{ads} \quad (5)$$

The ΔG_{ads} value for azo-Schiff **4** (–23.8 kJ/mol) indicates physisorption adsorption, because its value is a less negative value and is around –20 kJ/mol.[28–30]

4. Conclusion

By measuring the anti-corrosion properties of the azo-Schiff compound **4**, it was discovered that this is a more effective compound than the initial azo compound **3**. This is likely because **4** contains additional heteroatoms, which are able to donate unpaired electrons to metals and inhibit corrosion.

Supplementary Material

FT-IR of azo compound **3** and azo-Schiff derivative **4**, MS spectrum of **3** and UV-Vis spectra of **3** and **4**.

Declaration of competing interest

The authors declare that they have no conflict of interest.

This study was not supported by any organization.

5. References

1. M. Abdulhussin Enad, M. Y. Kadhim, A. S. Abdulnabi, *J. Glob. Pharma Technol.* **2020**, *12*, 651–656.
2. M. S. Mezhr, *Ann. Rom. Soc.* **2021**, 910–928. **DOI:**10.1088/1757-899X/928/2/022037
3. H. Khaleel, A. A. Ateeq, A. A. Ali, *Int. J. Appl. Eng. Res.* **2018**, *13(6)*, 3638–3647.
4. S. Bashir, V. Sharma, H. Lgaz, I. M. Chung, A. Singh, *J. Mol. Liq.* **2018**, *263*, 454–462. **DOI:**10.1016/j.molliq.2018.04.143
5. A. Nasima, A. K. Singh, B. Chugh, M. Akram, F. Perveen, I. Rasheed, F. Altaf, P. A. Channar, A. Saeed, *Ionics* **2019**, *25*, 5057–5075. **DOI:**10.1007/s11581-019-03028-y
6. I. B. Obot, S. A. Umoren, N. K. Ankah, *J. Mol. Liq.* **2019**, *277*, 749–761. **DOI:**10.1016/j.molliq.2018.12.108
7. A. K. Singh, S. Thakur, B. Pani, G. Singh, *New J. Chem.* **2018**. *42(3)*, 2113–2124. **DOI:**10.1039/C7NJ04162D
8. R. Yıldız, *Ionics.* **2019**, *25(2)*, 859–870. **DOI:**10.1007/s11581-018-2649-5
9. H. M. Elabbasy, H. S. Gadow, *J. Mol. Liq.* **2021**, *321*, 114918. **DOI:**10.1016/j.molliq.2020.114918
10. H. S. Gadow, M. Fakeeh, *RSC Adv.* **2022**, *12(15)*, 8953–8986. **DOI:**10.1039/D2RA01296K

11. T. E. Schmitzhaus, M. R. Vega, R. Schroeder, I. L. Muller, Mattedi, C. F. Malfatti, *Corros. Mater*. **2020**, *71(7)*, 1175–1193. **DOI:**10.1002/maco.201911347
12. O. O. Ogunleye, A. O. Arinkoola, O. A. Eletta, O. O. Agbede, Y. A. Osho, A. F. Morakinyo, J. O. Hamed, *Heliyon*. **2020**, *6(1)*, e03205. **DOI:**10.1016/j.heliyon.2020.e03205
13. I. Danaee, S. Ramesh Kumar, M. Rashvand Avei, M. Vijayan, *Mater. Res*. **2020**, *23*, e20180610.
14. H. S. Gadow, M. Fakeeh, *RSC Adv*. **2022**, *12(15)*, 8953–8986. **DOI:**10.1039/D2RA01296K
15. M. E. Moustafa, A. I. Ali, A. Y. El-Etre, H. A. Ibrahim, *Benha. J. Appl. Sci*. **2019**, *4(2)*, 167–187. **DOI:**10.21608/bjas.2019.187205
16. P. Kumari, M. Lavanya, *J. Bio- Tribo-Corros*. **2021**, *7(3)*, art. no. 110. **DOI:**10.1007/s40735-021-00542-3
17. D. Clofent, M. de Homdedeu, M. Muñoz-Esquerre, M. J. Cruz, X. Muñoz *Allergy Asthma Clin. Immunol.* **2020**, *16*, art. no. 7. **DOI:**10.1186/s13223-020-0404-8
18. F. Vázquez-Ortega, I. Lagunes, Á. Trigos, *Dyes Pigments*, **2020**, *176*, 108248. **DOI:**10.1016/j.dyepig.2020.108248
19. L. H. Madkour, S. Kaya, L. Guo, C. Kaya, *J. Mol. Struct*. **2018,** *1163*, 397–417. **DOI:**10.1016/j.molstruc.2018.03.013
20. H. M. Alabidi, A. M. Farhan, N. S. Salh, A. A. J. Aljanaby, *Curr. Appl. Sci. Technol*. **2023**, *23(4),* art. no. 7.
21. M. H. Yusoff, M. N. Azmi, M. H. Hussin, H. Osman, P. B. Raja, A. Abdul Rahim, K. Awang, *Int. J. Electrochem. Sci*, **2020**, *15(12)*, 11742–11756. **DOI:**10.20964/2020.12.43
22. A. Madani, L. Sibous, A. Hellal, I. Kaabi, E. Bentouhami, *J. Mol. Struct*. **2021**, *1235*, 130224. **DOI:**10.1016/j.molstruc.2021.130224
23. H. M. Alabidi, A. M. Farhan, M. M. Al-Rufaie, *Curr. Appl. Sci. Technol*. **2021,** 176–187.
24. H. M. Alabidi, A. M. Farhan, H. M. Y. Al-Laban, A. A. J. Aljanaby, *Egypt. J. Chem*. **2023**, *66(1)*, 175–181.
25. N. A. Abdul-Rida, A. M. Farhan, N. A. Al-Masoudi, B. A. Saeed, D. Miller, M. F. Lin, *Mol. Divers*. **2021**, *25*, 661–671. **DOI:**10.1007/s11030-020-10038-w
26. N. A. AL-Rida, A. M. Farhan, *J. Phys. Conf. Ser*. **2019**, *1294, 5*, 052002. **DOI:**10.1088/1742-6596/1294/5/052002
27. S. Benkhaya, S. M'rabet, A. El Harfi, *Heliyon* **2020**, *6*, e03271. **DOI:**10.1016/j.heliyon.2020.e03271
28. A. Singh, K. R. Ansari, J. Haque, P. Dohare, H. L. Gaz, R. Salghi, M. A. Quraishi, *J. Taiwan Inst. Chem. Eng*. **2018**, *82*, 233–251. **DOI:**10.1016/j.jtice.2017.09.021
29. C. Verma, L. O. Olasunkanmi, E. E. Ebenso, M. A. Quraishi, *J. Mol. Liq* **2018**, *251*, 100–118. **DOI:**10.1016/j.molliq.2017.12.055
30. P. Singh, E. E. Ebenso, L. O. Olasunkanmi, I. B. Obot, M. A. Quraishi, *J. Phys. Chem. C*. **2016**, *120(6)*, 3408–3419. **DOI:**10.1021/acs.jpcc.5b11901

Povzetek

Pripravili smo dve novi spojini: azo spojino **3** [2-((4-hidroksi-3-(*E*)-(2-hidroksi-5-nitrofenil)diazenil)benzaldehid] ter njen Schiffov derivat **4** [2-((4-hidroksi-3-((*E*)-(2-hidroksi-5-nitrofenil)diazenil)benziliden)amino)-4-nitrofenol] (azo-Schiff **4**). Za karakterizacijo novih spojin smo uporabili ^{13}C-NMR, ^{1}H-NMR, FT-IR, masno spektroskopijo in UV-Vis analizo. Novo, sintetizirano azo-Schiffovo spojino **4** smo v nizkih koncentracijah (0.001–0.006 M) uporabili kot inhibitor korozije mehkega jekla (MS). Študije izgube mase v 1 M HCl pri 298 K so pokazale, da azo-Schiffova spojina **4** izkazuje dobro protikorozijsko učinkovitost, t.j. 75 % pri njeni koncentraciji 0.002 M. Ugotovili smo, da adsorpcija poteka skladno z Langmuirjevo izotermo, kjer je ΔG približno –23.8 kJ/mol, kar potrjuje, da s fizično adsorpcijo preiskovane spojine na mehko jeklo nastane stabilen zaščitni sloj.